



On Self-Organization Structure for Fluid Dynamical Systems via Solitary Waves

H.M. Tenkam^{1*}, E.F. Doungmo Goufo² and S. Kumar³

¹ *Department of Mathematics and Applied Mathematics, North-west University, Private Bag X6001 Potchefstroom, 2520 South Africa.*

² *Department of Mathematical Sciences, University of South Africa, Florida Campus, 0003 South Africa.*

³ *Department of Mathematics, National Institute of Technology, Jamshedpur, 831014 India.*

Received: March 11, 2021; Revised: September 23, 2021

Abstract: The process of self-organization occurs and is used in many aspects of life with applications found in domains of biological, physical and machining systems. Finding ways to create this kind of processes has attracted the interest of many scientists around the world. We combine in this paper some mathematical concepts to model and generate the self-organization process happening in wave motion. We make use of the Harry Dym system together with the fractal and fractional operators. The resulting model is solved numerically and its stability results are provided. Numerical simulations show the combined system involved in a self-organization dynamic with the replication of the initial objects and the formation of subsequent fractal patterns which vary with the fractional operator. The results prove that we are in the presence of a system capable of artificially structuring fractals using mathematical concepts, numerical techniques, codes and simulations.

Keywords: *mathematical models; self-organization process; numerical simulation; fractal-fractional structures.*

Mathematics Subject Classification (2010): 70K75, 28A80, 26A33, 33F05, 93-00.

* Corresponding author: <mailto:michel.djouosseutenkam@nwu.ac.za>

1 Introduction

The self-organization process is found in many natural structures and represents the main concept of the Systems Science field. It sometimes refers to the formation of various patterns in some physical and biological systems. For instance, we can see it in the rippled dune formation in a sand desert or in the cells combination that creates highly structured and ordered tissues. In most of these systems, the order and structure are acquired thanks to the proximate means characterizing them. It is then possible to view the pattern formation at the global level of the structure due to interactions between components of lower levels. The whole process is specifically governed by natural selection characterizing physical and biological systems. However, some other systems (found in nature) can become organized due to external commands, for instance, human interventions (protocols, algorithms, simulations) that lead to the building of sophisticated societies, structures or machines. We are exploring the later case with the specific domain of wave-motion where the model of Harry Dym is considered [1–8].

It is important to recall that the self-organization process is closely related to the dynamical system theory. A number of dynamical systems have been investigated several times in the course of science history, but the concept remains fascinating for scientists. One of the reasons is the unpredictable trajectories that characterize the vast amount of applications found in engineering, physics, biology, (applied) mathematics, and medical sciences [4, 9–12, 14]. A simple example includes the study of chaotic systems with complicated bifurcations that exist there. The literature comprises diverse types of dynamical systems [10, 11, 13–15], namely, the classical dynamical system and also the open dynamical system. The later can be seen in Fig.1, where different orbits and trajectories can be observed. It starts with the initial trajectories (Fig.1 (upper right)) of an agent dynamical system in isolation in its suitable space \mathcal{S}_π . The process goes on with a decoupled agent dynamical system, see Fig.1 (upper left), well defined on its suitable total space \mathfrak{S}_τ and which joints together to form the total system shown in Fig.4 (lower left). The system is completed by the projection or paths, see Fig.1 (lower right), showing how an agent behaves in a particular environment (\mathcal{S}_π). The behavior of the system in this last space (\mathcal{S}_π) is the major symbolism at the core of the so-called open dynamical system as it contrasts with the agent in isolation (Fig.1 (upper right)). Particularly, the orbits in the open phase portrait for the embedded agent dynamical system (Fig.1 (lower right)) overlap, which is not the case for those of the agent in isolation (Fig.1 (upper right)). This is what makes open dynamical systems generally hard to study. This statement is supported by the types of dynamics observed in complex systems like fractals. Some of these dynamics are depicted in Fig.2 and Fig.3. These representations show different sorts of waves involved in fractal-type motifs. The fractal patterns are artificially (numerically) formed due to mathematical simulations issued from modeling the type of movements observed in nature around us. The fractal motif include sound-type fractal waves, heat-type fractal waves, particle fractal waves, ocean chaotic fractal waves, spiral wave fractal swirls, fluffy cloud chaotic fractal wave spirals, chaotic fractal light waves and so on.

1.1 Approximation results for the classical Harry Dym model

Let $\Omega = (a, b)$, $\mathbb{R} \ni T > 0$ $\mathbb{R} \ni b > a \in \mathbb{R}$ and $g \in C^0 [[0, T] \times \Omega]$. Let $\alpha \in [0; 1]$, $\beta \in (0, +\infty)$, then consider the non-linear Dym equation in its classical form. Existence and uniqueness of the exact solution are shown for the model under investigation that reads

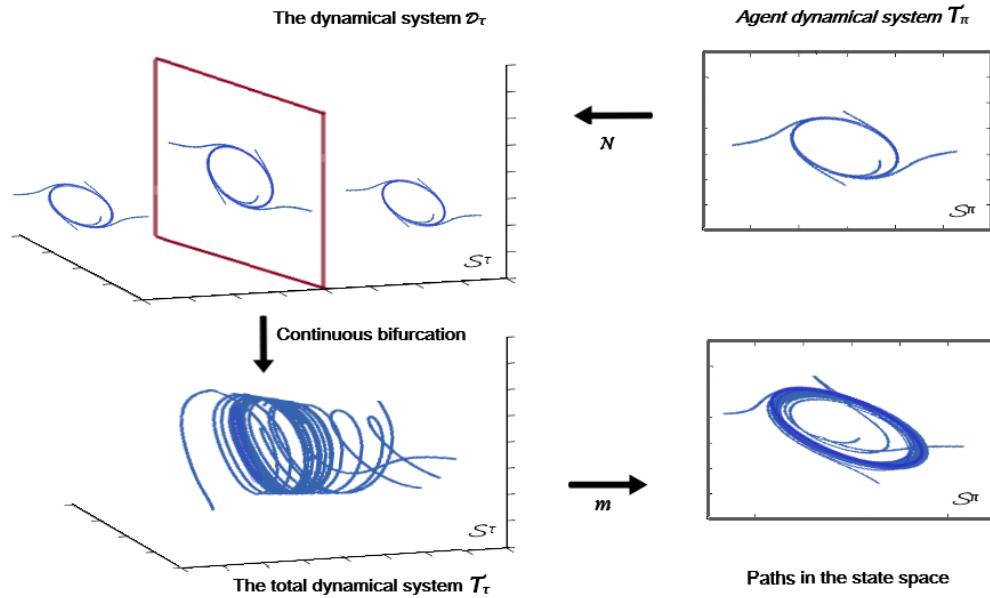


Figure 1: Basic principle of the open dynamical system. We can see the initial trajectories (upper right) of an agent dynamical system in isolation in its suitable space S_π . The process goes on with a decoupled agent dynamical system (upper left), well defined on its suitable total space S_τ and which joints together to form the total system shown (lower left). The system is completed by the projection or paths (lower right) showing how an agent behaves in a particular environment (S_π). The behavior of the system in this last space (S_π) is the major symbolism at the core of the so-called open dynamical system as it contrasts with the agent in isolation (upper right). Particularly, the orbits in the open phase portrait for the embedded agent dynamical system (lower right) overlap, which is not the case for those of the agent in isolation (upper right).

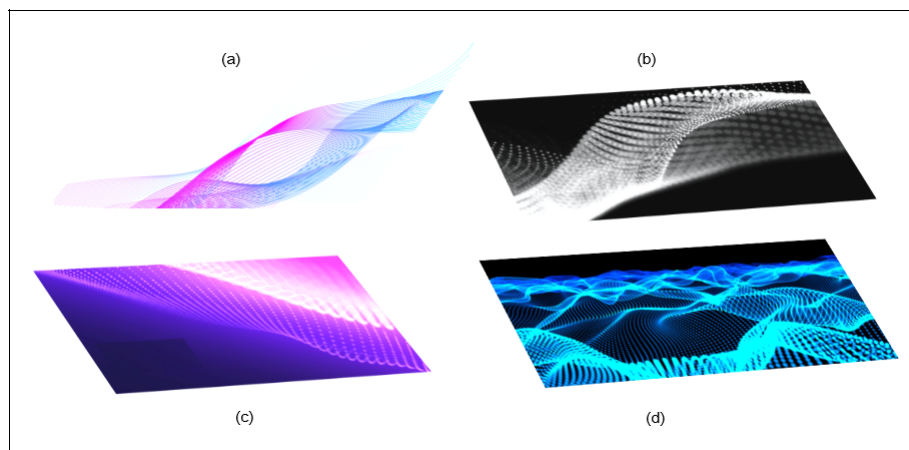


Figure 2: Simulation showing different sorts of waves involved in fractal-type motifs. The fractal patterns here are artificially (numerically) formed due to mathematical simulations issued from modeling the type of movements observed in nature. In (a) we have sound fractal waves, in (b) heat fractal waves, in (c) particle fractal wave and (d) ocean chaotic fractal wave.

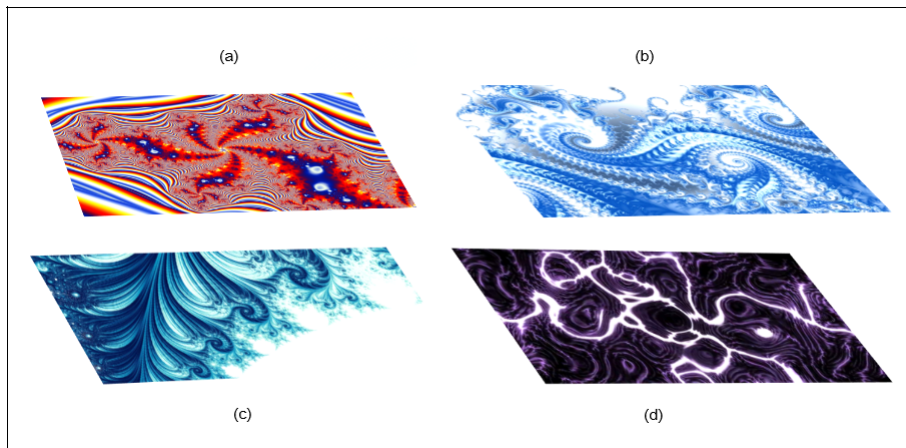


Figure 3: Simulation showing different sorts of waves involved in fractal-type patterns. The fractal motifs here are artificially (numerically) formed due to mathematical simulations issued from modeling the type of movements observed in nature. In (a) fractal wave multi color motion glowing lines, in (b) spiral wave fractal swirl, (c) fluffy cloud chaotic fractal wave spirals, in (d) chaotic fractal light waves.

as

$$\frac{\partial}{\partial t}g(t, x) = g^3g_{xxx}(t, x), \quad (1)$$

subject to the initial condition

$$g(0, x) = g_0(x) \quad (2)$$

with $g : \Omega \mapsto \mathbb{R}_+$.

The function g can be approximated in the form

$$g(t, x) = \sum_{j=0}^{\infty} e_j \mathbf{H}_j(x), \quad (3)$$

here the coefficients e_j are given by

$$e_j = 2^k \int_0^1 g(t, x) \mathbf{H}_j(x) dx, \quad (4)$$

where $j = 2^k + l$, $k \geq 0$ and $0 \leq l < 2^k$. Moreover, the x -dependant function $\mathbf{H}_j(x)$ is the Haar wavelet function [1, 9, 16–18]

$$\mathbf{H}_j(x) = \begin{cases} 1, & \text{if } \frac{l}{p} \leq x < \frac{l+1/2}{p}; \\ -1, & \text{if } \frac{l+1/2}{p} \leq x < \frac{l+1}{p}; \\ 0, & \text{elsewhere} \end{cases} \quad (5)$$

with $p = 2^k$, $k = 1, 2, \dots, L$, where L denotes the chosen resolution's level and l represents the translation parameter which can take the values $0, 1, \dots, p - 1$. Because the

series of function $g(t, x)$ comprises an infinite number of terms, it can be obtained using the following definite sum:

$$g(t, x) = \sum_{j=0}^{p-1} e_j \mathbf{H}_j(x), \tag{6}$$

which takes the form

$$g(t, x) = {}^t \mathbf{e}_p \mathbf{H}_p(x)$$

with ${}^t \mathbf{e}_p$ being the transpose of

$$\mathbf{e}_p = \begin{pmatrix} e_0 \\ e_1 \\ \vdots \\ e_{p-1} \end{pmatrix} \quad \text{and} \quad \mathbf{H}_p = \begin{pmatrix} \mathbf{H}_0 \\ \mathbf{H}_1 \\ \vdots \\ \mathbf{H}_{p-1} \end{pmatrix}.$$

Now, using the Haar wavelet technique to solve the model (1) and (2), we can assume that the t -partial derivative $\frac{\partial g_{xxx}}{\partial t}(t, x)$ is expandable as follows:

$$\frac{\partial g_{xxx}}{\partial t}(t, x) = \sum_{j=0}^{2P} e_j \mathbf{H}_j(x), \quad t_r < t \leq t_{r+1}, \tag{7}$$

where $2P$ is the number of collocation points calculated as

$$x_i = \frac{i - 1/2}{2P}, \quad \text{with } i = 1, 2, \dots, 2P. \tag{8}$$

Integration of (7) respectively with respect to variables t and x leads to

$$g_{xxx}(t, x) = g_{xxx}(t_r, x) + (t - t_r) \sum_{j=1}^{2P} e_j \mathbf{H}_j(x),$$

$$g_{xx}(t, x) = g_{xx}(t, 0) - g_{xx}(t_r, 0) + g_{xx}(t_r, x) + (t - t_r) \sum_{j=1}^{2P} e_j \mathbf{M}_1^j(x)$$

and

$$g_x(t, x) = g_x(t, 0) - g_x(t_r, 0) + g_x(t_r, x) + x[g_{xx}(t, 0)] - g_{xx}(t_r, 0) + (t - t_r) \sum_{j=1}^{2P} e_j \mathbf{M}_2^j(x),$$

which finally leads to

$$\begin{aligned} g(t, x) &= g(t, 0) + g(t_r, x) - g(t_r, 0) + x[g_x(t, 0) - g_x(t_r, 0)] \\ &+ \frac{x^2}{2}[g_x(t, 1) - g_x(t, 0) + g_x(t_r, 0) - g_x(t_r, 1)] \\ &(t - t_r) \sum_{j=1}^{2P} e_j \left(-\frac{x^2}{2} \mathbf{M}_2^j(1) + \mathbf{M}_3^j(x) \right), \end{aligned} \tag{9}$$

where we have considered at the point $x = 1$ the operational matrix \mathbf{M} defined in its general expression for the indexes $j = l + p + 1$ by

$$\mathbf{M}_s^j(x) = \begin{cases} \frac{1}{s!}(x - l/p)^s, & \text{if } \frac{l}{p} \leq x < \frac{l+1/2}{p}; \\ \frac{1}{s!} \left[(x - l/p)^s - 2(x - \frac{l+1/2}{p})^s \right], & \text{if } \frac{l+1/2}{p} \leq x < \frac{l+1}{p}; \\ \frac{1}{s!} \left[(x - l/p)^s - 2(x - \frac{l+1/2}{p})^s + (x - \frac{l+1}{p})^s \right], & \text{if } \frac{l+1/2}{p} \leq x < \frac{l+1}{p}; \\ 0, & \text{elsewhere.} \end{cases} \quad (10)$$

The differentiation of (9) with respect to variable t is followed by the discretization at the point (t_r, x_i)

$$\begin{aligned} g(t_{r+1}, x_i) &= g(t_{r+1}, 0) + g(t_r, x_i) - g(t_r, 0) + x_i[g_x(t_{r+1}, 0) - g_x(t_r, 0)] \\ &\quad + \frac{x_i^2}{2}[g_x(t_{r+1}, 1) - g_x(t_{r+1}, 0) + g_x(t_r, 0) - g_x(t_r, 1)] \\ &\quad (t_{r+1} - t_r) \sum_{j=1}^{2P} e_j \left(-\frac{x_i^2}{2} \mathbf{M}_2^j(1) + \mathbf{M}_3^j(x_i) \right), \\ \frac{\partial g}{\partial t}(t_{r+1}, x_i) &= \frac{\partial g}{\partial t}(t_{r+1}, 0) + x_i \frac{\partial g_x}{\partial t}(t_{r+1}, 0) + \frac{x_i^2}{2} \left[\frac{\partial g_x}{\partial t}(t_{r+1}, 1) - \frac{\partial g_x}{\partial t}(t_{r+1}, 0) \right] \\ &\quad \sum_{j=1}^{2P} e_j \left(-\frac{x_i^2}{2} \mathbf{M}_2^j(1) + \mathbf{M}_3^j(x_i) \right). \end{aligned} \quad (11)$$

Still, using the discretization at the point (t_r, x_i) and the substitution into (1) leads to

$$\begin{aligned} &\sum_{j=1}^{2P} e_j \left(\frac{x_i^2}{2} \mathbf{M}_2^j(1) - \mathbf{M}_3^j(x_i) + g^3(t_r, x_i)(t_{r+1} - t_r) \mathbf{H}_j(x_i) \right) \\ &= \frac{\partial g}{\partial t}(t_{r+1}, 0) - g^3(t_r, x_i)g_{xxx}(t_r, x_i) + x_i \frac{\partial g_x}{\partial t}(t_{r+1}, 0) + \frac{x_i^2}{2} \left[\frac{\partial g_x}{\partial t}(t_{r+1}, 1) + \frac{\partial g_x}{\partial t}(t_{r+1}, 0) \right], \end{aligned} \quad (12)$$

equivalently,

$$\begin{aligned} &\sum_{j=1}^{2P} e_j \left(\frac{x_i^2}{2} \mathbf{M}_2^j(1) - \mathbf{M}_3^j(x_i) + g^3(t_r, x_i)(t_{r+1} - t_r) \mathbf{H}_j(x_i) \right) \\ &+ g^3(t_r, x_i)g_{xxx}(t_r, x_i) - \frac{1}{t_{r+1} - t_r} [g(t_{r+1}, 0) - g(t_r, 0)] - x_i \left[\frac{\partial g}{\partial t}(t_{r+1}, 0) - \frac{\partial g}{\partial t}(t_r, 0) \right] \\ &- \frac{x_i^2}{2(t_{r+1} - t_r)} \left[\left(\frac{\partial g}{\partial t}(t_{r+1}, 1) - \frac{\partial g}{\partial t}(t_r, 1) \right) - \left(\frac{\partial g}{\partial t}(t_{r+1}, 0) - \frac{\partial g}{\partial t}(t_r, 0) \right) \right] = 0, \end{aligned} \quad (13)$$

where we have used the scheme

$$\frac{\partial g}{\partial t}(t_{r+1}, 0) = \frac{1}{t_{r+1} - t_r} [g(t_{r+1}, 0) - g(t_r, 0)]$$

and

$$\frac{\partial g}{\partial t}(t_{r+1}, 1) = \frac{1}{t_{r+1} - t_r} [g(t_{r+1}, 1) - g(t_r, 1)].$$

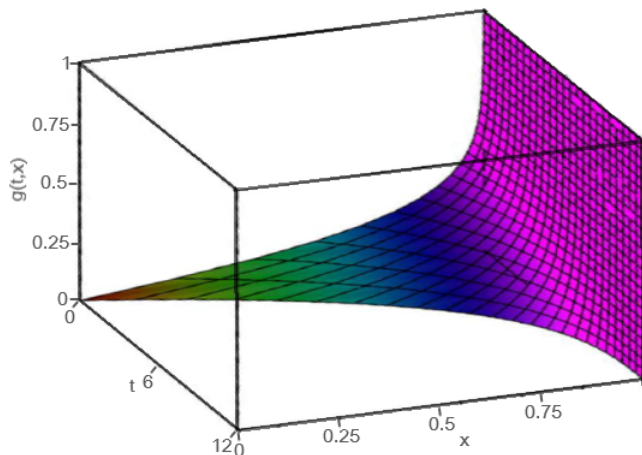


Figure 4: Three-dimensional representation of the solution $g(t, x)$ to model (1) and (2) when $g_0(x) = x^2$.

Hence, equation (13) allows the calculation of the Haar wavelet coefficients, which are used to establish the numerical solution (9). The related numerical simulations are depicted in Fig.1 to Fig.5 relating the usual wave dynamics with different given initial conditions.

1.2 Recent progress in self-organization operators

To help with the advancement of sciences and try to understand and describe many unsolved problems that were too complex to model, fractional derivatives were proposed. Those operators have since shown their infinite importance in applied sciences modelling. Today some authors classify them into two types: local and non-local [19–22]. Since the moment when Riemann and Liouville proposed their integral, from which derivatives of fractional were constructed, there has been a huge development in the domain with various and variant definitions proposed by a number of authors. In fact, the latest related literature comprises (but is not limited to) the following definitions.

Formerly:

- The Riemann–Liouville derivative ${}^{RL}D_t^\gamma$ with fractional order γ reads as

$${}^{RL}D_t^\gamma g(t, x) = \frac{1}{\Gamma(n - \gamma)} \left(\frac{d}{dt}\right)^n \int_0^t (t - v)^{n-\gamma-1} g(v, x) dv, \tag{14}$$

$$n - 1 < \gamma \leq n.$$

- The Caputo derivative ${}^C D_t^\gamma$ with fractional order γ reads as

$${}^C D_t^\gamma g(t, x) = \frac{1}{\Gamma(n - \gamma)} \int_0^t (t - v)^{n-\gamma-1} \left(\frac{d}{dv}\right)^n g(v, x) dv, \tag{15}$$

$$n - 1 < \gamma \leq n.$$

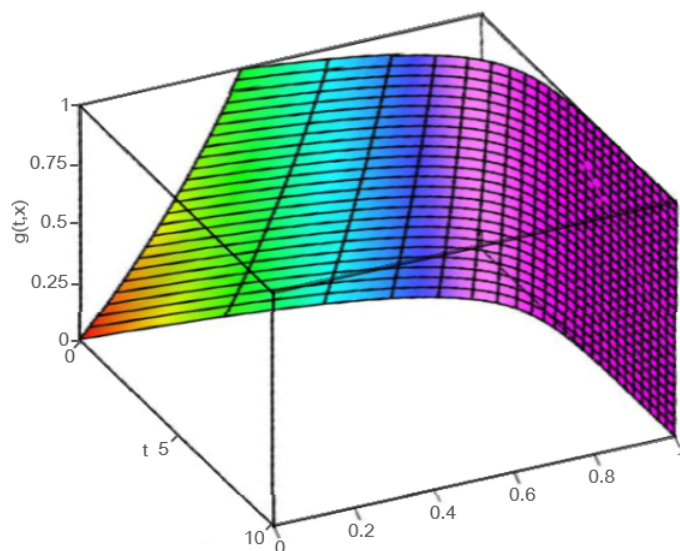


Figure 5: Three-dimensional representation of the solution $g(t, x)$ to model (1) and (2) when $g_0(x) = e^x - 1$.

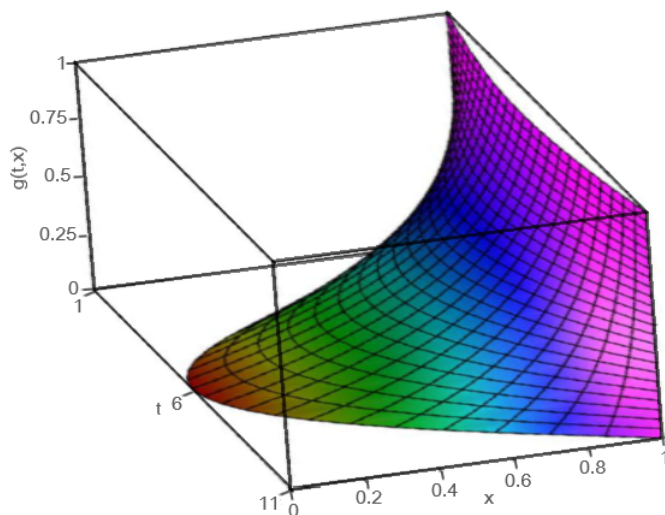


Figure 6: Three-dimensional representation of the solution $g(t, x)$ to model (1) and (2) when $g_0(x) = xe^x$.

More recently [14, 20, 23, 24]:

- The Caputo-Fabrizio derivative ${}^{CF}D_t^\gamma$ with fractional order γ reads as

$${}^{CF}D_t^\gamma g(t, x) = \frac{\mathbf{n}(\gamma)}{(1 - \gamma)} \int_0^t \frac{\partial g}{\partial v}(v, x) \exp(-\gamma(t - v)(1 - \gamma)^{-1}) dv, \quad (16)$$

where $\mathbf{n}(\gamma)$ satisfies

$$\mathbf{n}(0) = \mathbf{n}(1) = 1. \quad (17)$$

- The new-Riemann–Liouville derivative ${}^{nRL}D_t^\gamma$ with fractional order γ is given by

$${}^{nRL}D_t^\gamma g(t, x) = \frac{(2 - \gamma)\mathbf{n}(\gamma)}{2(1 - \gamma)} \frac{d}{dt} \int_0^t g(v, x) \exp(-\gamma(t - v)(1 - \gamma)^{-1}) dv. \quad (18)$$

- The Atangana-Baleanu-Caputo derivative ${}^{ABC}D_t^\gamma$ with fractional order γ reads as

$${}^{ABC}D_t^\gamma g(t, x) = \frac{\mathbf{n}(\gamma)}{(1 - \gamma)} \int_0^t \frac{\partial g}{\partial v}(v, x) E_\gamma[-\gamma(t - v)^\gamma(1 - \gamma)^{-1}] dv. \quad (19)$$

In the definitions here above, the function g is assumed to belong to the Sobolev space

$$S^1(\alpha, \beta) = \{g : g, \frac{\partial}{\partial t}g \in L^2(\alpha, \beta)\}. \quad (20)$$

- The Caputo-sense two-parameter derivative ${}^{CG}D_t^{\gamma, \theta}$ with fractional order γ , when knowing the parameter $\theta \in \mathbb{R}$, reads as

$${}^{CG}D_t^{\gamma, \theta} g(t, x) = \frac{\theta \tilde{\mathbf{n}}(\gamma, \theta)}{(\theta - \gamma)} \int_0^t \frac{\partial g}{\partial v}(v, x) (t - v)^{\theta - 1} E_{\gamma, \theta}[-\gamma\theta(t - v)^\gamma(\theta - \gamma)^{-1}] dv, \quad (21)$$

where $\theta \in \mathbb{R}$ and $\tilde{\mathbf{n}}(\gamma, \theta)$ verifies $\tilde{\mathbf{n}}(0, 1) = \tilde{\mathbf{n}}(1, 1) = 1$.

Introduction to fractal-fractional derivative

Initially defined to be the convolution operation between a fractal differential operator and the usual law functions found in fractional calculus, the fractal-fractional derivative [25] was introduced in order to attract and describe a huge number of non-local problems in real life while respecting the fractal structure that characterizes them. In the recent literature, one can find a number of versions for the definitions of fractal-fractional operation and this mainly depends on the kind of law function we choose to use. Some are given as follows.

Definition 1.1 We consider $\Omega \in \mathbb{R}^3$, $T \in \mathbb{R}$, and assume that $g(t, x)$ defined on $(0, T) \times \Omega$ is t -fractal differentiable with the order γ on the interval $(0, T)$, then:

1. The fractal-fractional derivative of g of order γ in the sense of Riemann-Liouville with the power law reads as

$${}^{FRP}D_t^\gamma g(t, x) = \frac{1}{\Gamma(1 - \gamma)} \frac{\partial}{\partial t^\gamma} \int_0^t g(\vartheta, x) (t - \vartheta)^{-\gamma} d\vartheta, \quad (22)$$

where $\frac{\partial}{\partial t^\gamma}g$ is defined as

$$\frac{\partial}{\partial t^\gamma}g(t, x_0) = \lim_{t \rightarrow t_0} \frac{g(t, x) - g(t, x_0)}{t^\gamma - t_0^\gamma}.$$

The generalized version of (22) is defined by

$${}^{FRP}D_t^{\gamma,\varsigma}g(t,x) = \frac{1}{\Gamma(1-\gamma)} \frac{\partial^\varsigma}{\partial t^\gamma} \int_0^t g(\vartheta,x) (t-\vartheta)^{-\gamma} d\vartheta, \quad (23)$$

with $\varsigma > 0$ and $\frac{\partial^\varsigma}{\partial t^\gamma}g$ given by

$$\frac{\partial^\varsigma}{\partial t^\gamma}g(t,x_0) = \lim_{t \rightarrow t_0} \frac{g^\varsigma(t,x) - g^\varsigma(t,x_0)}{t^\gamma - t_0^\gamma}.$$

Similarly, the Caputo version of this definition can be given.

2. The fractal-fractional derivative of g of order γ in the sense of Caputo with the power law reads as

$${}^{FCP}D_t^\gamma g(t,x) = \frac{1}{\Gamma(1-\gamma)} \int_0^t \frac{\partial}{\partial \vartheta^\gamma} g(\vartheta,x) (t-\vartheta)^{-\gamma} d\vartheta, \quad (24)$$

the generalized version is

$${}^{FCP}D_t^{\gamma,\varsigma}g(t,x) = \frac{1}{\Gamma(1-\gamma)} \int_0^t \frac{\partial^\varsigma}{\partial \vartheta^\gamma} g(\vartheta,x) (t-\vartheta)^{-\gamma} d\vartheta. \quad (25)$$

The following definitions are related to the exponential law.

3. The fractal-fractional derivative of g of order γ in the sense of Riemann-Liouville with the exponential law reads as

$${}^{FRE}D_t^\gamma g(t,x) = \frac{\mathbf{n}(\gamma)}{(1-\gamma)} \frac{\partial}{\partial t^\gamma} \int_0^t g(\vartheta,x) \exp\left(\frac{-\gamma(t-\vartheta)}{1-\gamma}\right) d\vartheta, \quad (26)$$

where $\mathbf{n}(0) = \mathbf{n}(1) = 1$, with

the generalized version

$${}^{FRE}D_t^{\gamma,\varsigma}g(t,x) = \frac{\mathbf{n}(\gamma)}{(1-\gamma)} \frac{\partial^\varsigma}{\partial t^\gamma} \int_0^t g(\vartheta,x) \exp\left(\frac{-\gamma(t-\vartheta)}{1-\gamma}\right) d\vartheta. \quad (27)$$

4. The fractal-fractional derivative of g of order γ in the sense of Caputo with the exponential law reads as

$${}^{FCE}D_t^\gamma g(t,x) = \frac{\mathbf{n}(\gamma)}{(1-\gamma)} \int_0^t \frac{\partial}{\partial \vartheta^\gamma} g(\vartheta,x) \exp\left(\frac{-\gamma(t-\vartheta)}{1-\gamma}\right) d\vartheta, \quad (28)$$

with the generalized version

$${}^{FCE}D_t^{\gamma,\varsigma}g(t,x) = \frac{\mathbf{n}(\gamma)}{(1-\gamma)} \int_0^t \frac{\partial^\varsigma}{\partial \vartheta^\gamma} g(\vartheta,x) \exp\left(\frac{-\gamma(t-\vartheta)}{1-\gamma}\right) d\vartheta. \quad (29)$$

The following definitions are related to the Mittag-Leffler law.

5. The fractal-fractional derivative of g of order γ in the sense of Riemann-Liouville with the Mittag-Leffler law reads as

$${}^{FRm}D_t^\gamma g(t, x) = \frac{\mathbf{n}(\gamma)}{(1-\gamma)} \frac{\partial}{\partial t^\gamma} \int_0^t g(\vartheta, x) E_\gamma \left(\frac{-\gamma(t-\vartheta)^\gamma}{1-\gamma} \right) d\vartheta, \tag{30}$$

where $\mathbf{n}(\gamma)$ is a regularization function. Here the generalized version is

$${}^{FRm}D_t^{\gamma, s} g(t, x) = \frac{\mathbf{n}(\gamma)}{(1-\gamma)} \frac{\partial^s}{\partial t^\gamma} \int_0^t g(\vartheta, x) E_\gamma \left(\frac{-\gamma(t-\vartheta)^\gamma}{1-\gamma} \right) d\vartheta. \tag{31}$$

6. Then the fractal-fractional derivative of g of order γ in the sense of Caputo with the Mittag-Leffler law reads as

$${}^{FCm}D_t^\gamma g(t, x) = \frac{\mathbf{n}(\gamma)}{(1-\gamma)} \int_0^t \frac{\partial}{\partial \vartheta^\gamma} g(\vartheta, x) E_\gamma \left(\frac{-\gamma(t-\vartheta)^\gamma}{1-\gamma} \right) d\vartheta, \tag{32}$$

where $\mathbf{n}(\gamma)$ is a regularization real function related to the definition and with the more general version given as

$${}^{FCm}D_t^{\gamma, s} g(t, x) = \frac{\mathbf{n}(\gamma)}{(1-\gamma)} \int_0^t \frac{\partial^s}{\partial \vartheta^\gamma} g(\vartheta, x) E_\gamma \left(\frac{-\gamma(t-\vartheta)^\gamma}{1-\gamma} \right) d\vartheta. \tag{33}$$

Remark 1.1 In this analysis, we make use of the operator given by (26). To proceed, we have to associate to it another great concept, its associated fractal-fractional operator. Whence, we define the fractal-fractional integral of order γ , associated to (26), as follows:

$${}^{FRE}I_t^\gamma g(t, x) = \frac{\gamma(1-\gamma)t^{\gamma-1}g(t, x)}{\mathbf{n}(\gamma)} + \frac{\gamma^2}{\mathbf{n}(\gamma)} \int_0^t v^{\gamma-1}g(v)dv, \quad t > 0. \tag{34}$$

2 Self-Organization Process for Harry Dym Model

2.1 Stability of the fractal Dym model

In this section we consider the following system:

$${}^{FRE}D_t^\gamma g(t, x) = g^3 g_{xxx}(t, x), \tag{35}$$

subject to the initial condition

$$g(0, x) = g_0(x), \tag{36}$$

where we have combined the Dym model with the fractal-fractional derivative [25, 26], recalled to be defined in (26) as

$${}^{FRE}D_t^\gamma g(t, x) = \frac{\mathbf{n}(\gamma)}{(1-\gamma)} \frac{\partial}{\partial t^\gamma} \int_0^t g(\vartheta, x) \exp \left(\frac{-\gamma(t-\vartheta)}{1-\gamma} \right) d\vartheta, \tag{37}$$

where $\mathbf{n}(0) = \mathbf{n}(1) = 1$. To proceed further in the analysis, the fractal-fractional operator (37) should be associated with its anti-derivative called the fractal-fractional integral of order γ , and given by

$${}^{FF}I_t^\gamma g(t, x) = \frac{\gamma}{\Gamma(\gamma)} \int_0^t \varpi^{-\gamma} g(\mathbf{x}, \varpi) (t-\varpi)^{\gamma-1} d\varpi, \quad t > 0. \tag{38}$$

We have solved the classical model in Subsection 1.1 using the Haar wavelet method, which has provided a comprehensive analysis of the system and a global picture of the dynamic in the absence of the fractal influence. We are now using the Legendre wavelets method ([27, 28]) to solve the fractal-fractional system (35)–(36). Hence, we can transform it into a compact form with the application of the associated fractional integral on both sides of the model to have

$${}^{FF}D_t^\gamma g(t, x) = {}^T M_m \Psi_m(t), \quad (39)$$

where the matrix $\Psi_m(t)$ is given with the elements defining the Legendre wavelets which are expressed by

$$\psi_{nm}(t) = \begin{cases} 2^{l/2} \sqrt{2m+1} L_m^*(2^l t - n), & \text{if } t \in [\frac{n}{2^l}, \frac{n+1}{2^l}]; \\ 0, & \text{elsewhere.} \end{cases} \quad (40)$$

Recall that the shifted Legendre polynomial, given by L_m^* , is defined on $[0, 1]$ by $L_m^*(t) = L_m(2t - 1)$, with $(L_m(2t - 1))_m$ representing the family

$$L_0 = 1, \quad L_1 = x, \quad L_{m+1}(x) = \frac{1+2m}{m+1} x L_m(x) - \frac{m}{1+m} L_{m-1}(x), \quad m = 1, 2, \dots, N-1. \quad (41)$$

Recall also that we have considered $\mathbb{N} \ni J$ points $x = x_1, x_2, \dots, x_J$ and N is a positive integer number, $n = 1, 2, \dots, 2^l - 1$ and $l = 0, 1, 2, \dots$. $M_m = {}^T [\mathbf{m}_m^1, \mathbf{m}_m^2, \dots, \mathbf{m}_m^m]$ are coefficients to be found with ${}^T M_m$ being the transpose of the matrices M_m , respectively. Associating the initial conditions yields

$$g(t, x_j) \approx {}^T M_m Q_{m \times m}^\gamma \Psi_m(t) + g_0(x_j), \quad (42)$$

where $Q_{m \times m}^\gamma$ is the Legendre operational matrix of integration and the subscript m denotes its dimension. We know that [27, 28] that the Legendre wavelets can be expanded into an m -term form as

$$\Psi_m(t) = \Upsilon_{m \times m} A_m(t), \quad (43)$$

where $A_m(t) = {}^T [a_1(t), a_2(t), \dots, a_m(t)]$ are the block pulse functions so that

$$a_l(t) = \begin{cases} 1, & \text{if } t \in [\frac{l-1}{m}, \frac{l}{m}]; \\ 0, & \text{elsewhere} \end{cases} \quad (44)$$

for each $l = 1, 2, \dots, m$, and Υ is the Legendre wavelet matrix

$$\Upsilon_{m \times m} = \left[\Psi_m \left(\frac{1}{2m} \right) \Psi_m \left(\frac{3}{2m} \right) \cdots \Psi_m \left(\frac{2m-1}{2m} \right) \right].$$

Now the substitution of (43) into system (42) leads to

$$g(t, x_j) \approx {}^T M_m^1 Q_{m \times m}^\gamma \Upsilon_{m \times m} A_m(t) + [[g_0(x_j)]_i] A_m(t), \quad (45)$$

where

$$[[g_0(x_j)]_i] = [[g_0(x_j)]_1, g_0(x_j)]_2, \dots, g_0(x_j)]_m].$$

Now let

$${}^T M_m^i Q_{m \times m}^\gamma \Upsilon_{m \times m} = \mathcal{M}_{1 \times m}^{\gamma, i} = [\mathbf{m}_1^{\gamma, i}, \mathbf{m}_2^{\gamma, i}, \dots, \mathbf{m}_m^{\gamma, i}]. \tag{46}$$

Now the use of the collocations points $t_i = \frac{2i-1}{2^{l+1}N}$, $i = 1, 2, 3, \dots, m$, $N \in \mathbb{N}$, to disperse t and the substitution of (45) and (46) into the system (35) lead to

$$\begin{aligned} {}^T M_m^1 \Upsilon_{m \times m} &= \frac{x_i^2}{2} \mathcal{M}_{1 \times m}^{\gamma, i}(1) - \mathcal{M}_{1 \times m}^{\gamma, i}(x_i) + g^3(t_r, x_i)(t_{r+1} - t_r) \Upsilon_{1 \times m}(x_i) \\ &+ [\mathbf{m}_1^{\gamma, 2}, \mathbf{m}_2^{\gamma, 2}, \dots, \mathbf{m}_m^{\gamma, 2}]^T [\mathbf{m}_1^{\gamma, j}, \mathbf{m}_2^{\gamma, j}, \dots, \mathbf{m}_m^{\gamma, j}] \\ &+ [[g_0(x_j)]_1, [g_0(x_j)]_2, \dots, [g_0(x_j)]_m]. \end{aligned} \tag{47}$$

Hence, we obtain this non-linear system of equations with $3m$ unknown coefficients $\mathbf{m}_l^{\gamma, i}$, $1 \leq i \leq 3$, $1 \leq l \leq m$, which are easily found using the Newton iteration method. Then exploiting the model (42) leads to the expected numerical solution $(g(t, x))$.

2.2 Error analysis

Consider $\mathbb{N} \ni J$ points $x = x_1, x_2, \dots, x_J$. We assume here that the solution $g = g(t, x_i)$ is a function whose second order derivative with respect to t is bounded as

$$\left| \frac{\partial^2 g}{\partial t^2} \right| \leq \alpha_0^1.$$

Making use of the Legendre wavelet schemes described here above to approximate the solution $g(t, x_i)$ means it can be expanded as a uniformly convergent series that reads as

$$g(t, x_i) = \sum_{n=0}^{\infty} \sum_{m=0}^{\infty} \mathbf{m}_{nm}^{\gamma, 1} \psi_{nm}(t)$$

with

$$\mathbf{m}_{nm}^{\gamma, 1} = \langle g(t, x_i), \psi_{nm}(t) \rangle. \tag{48}$$

We have the following convergence results.

Proposition 2.1 *Let $i = 1, 2, \dots, J \in \mathbb{N}$ and $\alpha_0^1 > 0$. Assume that the solution $g(t, x_i)$ is a continuous function on $[0, T]$ whose second order derivative with respect to t is bounded as*

$$\left| \frac{\partial^2 g}{\partial t^2} \right| \leq \alpha_0^1,$$

then the coefficients $\mathbf{m}_{nm}^{\gamma, 1}$ satisfy

$$|\mathbf{m}_{nm}^{\gamma, 1}| < \frac{(12)^{1/2} \alpha_0^1}{(2m - 3)^2 (\sqrt{2n})^5}.$$

Proof. For $i \in \mathbb{N}$, let us consider the function $g = g(t, x_i)$ and using the definition of the Legendre wavelet coefficients given in (48) and taking into account (40), we have

$$\begin{aligned} \mathbf{m}_{nm}^{\gamma,1} &= \int_0^1 g(t, x_i) \psi_{nm}(t) dt \\ &= \int_{\frac{n}{2^l}}^{\frac{n+1}{2^l}} g(t, x_i) 2^{l/2} \sqrt{2m+1} L_m^*(2^l t - n) dt \\ &= \sqrt{\frac{1+2m}{2^l}} \int_0^1 g\left(\frac{n+\xi}{2^l}, x_i\right) L_m^*(\xi) d\xi \\ &\text{(where we have changed the variable as } t = \frac{n+\xi}{2^l}\text{)} \\ &= \sqrt{\frac{1}{(2m+1)2^{3l+2}}} \int_0^1 \frac{\partial g}{\partial t}\left(\frac{n+\xi}{2^l}, x_i\right) (L_{m+1}^*(\xi) - L_{m-1}^*(\xi)) d\xi \\ &= \sqrt{\frac{1}{(2m+1)2^{5l+2}}} \int_0^1 \frac{\partial^2 g}{\partial t^2}\left(\frac{n+\xi}{2^l}, x_i\right) \left(\frac{L_{m+2}^*(\xi) - L_m^*(\xi)}{6+4m} - \frac{L_m^*(\xi) - L_{m-2}^*(\xi)}{-2+4m}\right) d\xi, \end{aligned}$$

where we have used the derivative properties of the shifted Legendre polynomials [27, 28]. Hence

$$\begin{aligned} |\mathbf{m}_{nm}^{\gamma,1}| &\leq \left| \sqrt{\frac{1}{(2m+1)2^{5l+2}}} \right| \\ &\int_0^1 \left| \frac{\partial^2 g}{\partial t^2}\left(\frac{n+\xi}{2^l}, x_i\right) \right| \left| \left(\frac{L_{m+2}^*(\xi) - L_m^*(\xi)}{6+4m} - \frac{L_m^*(\xi) - L_{m-2}^*(\xi)}{-2+4m}\right) \right| d\xi. \end{aligned} \tag{49}$$

Developing the right-hand side of the inequality and making use of the constraint property $|x''(t)| \leq \alpha_0^1$ and the orthogonality property of the shifted Legendre polynomials finally lead to

$$|\mathbf{m}_{nm}^{\gamma,1}| \leq \sqrt{\frac{1}{\sqrt{2m+1}}} \cdot \frac{1}{2^{(5/2)l+1}} \cdot \alpha_0^1 \cdot \sqrt{\frac{\sqrt{3}}{(2m-3)}} \cdot \frac{1}{2m-1} < \frac{(12)^{1/2} \alpha_0^1}{(2m-3)^2 (\sqrt{2n})^5},$$

and the proposition is concluded. This result leads to the following error estimate.

Corollary 2.1 *Let $i = 1, 2, \dots, J \in \mathbb{N}$ and $\alpha_0^1 > 0$. Assume that the solution $g(t, x_i)$ is a continuous function on $[0, 1]$ whose second order derivative with respect to t is bounded as*

$$\left| \frac{\partial^2 g}{\partial t^2} \right| \leq \alpha_0^1,$$

then the error made when $g_{kN} = \sum_{n=0}^{2^l-1} \sum_{m=0}^{N-1} \mathbf{m}_{nm}^{\gamma,1} \psi_{nm}(t)$ approximates $g(t, x_i)$ satisfies

$$\Delta_{kN}^1 < (12)^{1/2} \alpha_0^1 \sqrt{\sum_{n=2^l}^{\infty} \sum_{m=N}^{\infty} \frac{1}{32n^5(2m-3)^4}}.$$

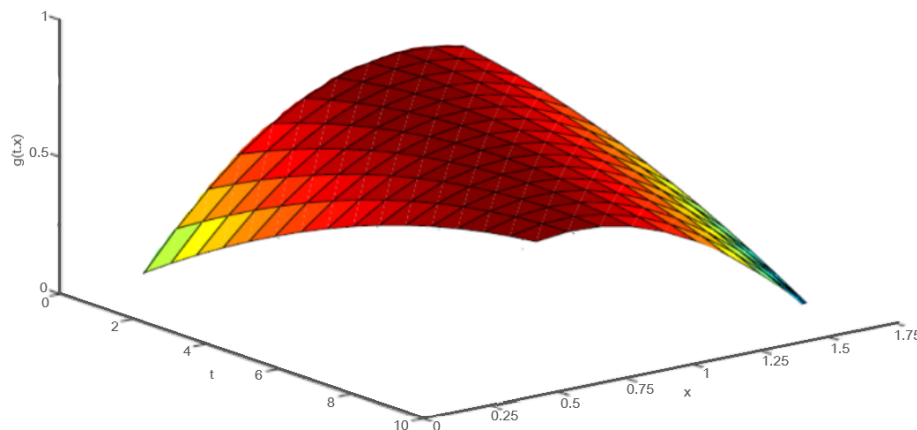


Figure 7: Three-dimensional representation of the solution $g(t, x)$ to model (35)–(36) when $g_0(x) = \frac{6}{10}e^x$ and $\gamma = 1$.

2.3 Numerical applications

Now, having solved the model and shown its stability results, we perform in this section some numerical simulations showing the behavior of the fractal-fractional system (35)–(36). The graphs in Fig.7 to Fig.12 show such behavior in three-dimensional and two-dimensional space. In Fig.7, we can see the three-dimensional representation of the solution $g(t, x)$ when $\gamma = 1$ with $g_0(x) = \frac{6}{10}e^x$. The two-dimensional representation is depicted in Fig.8. For $\gamma = 0.85$, the behavior of the solution $g(t, x)$ changes as depicted in Fig.9 – Fig.10 in three and two dimensions, respectively. The dynamic becomes involved in a self-organization process. This process consists of structuring itself in such a manner that the initial object is replicated approximately exactly to itself or to a part of itself. The process continues with the self-organization process which expands and multiplies in a similar way, for $\gamma = 0.65$, as shown in Fig.11 – Fig.12. Briefly, the system is shown to create diverse pattern formation processes, in this case, very important in the wave-motion domain. Thus, the system is capable of artificially structuring the fractals using mathematical concepts, numerical techniques, codes and simulations.

3 Concluding Remarks

We have combined some mathematical concepts and been able to model, solve and simulate a self-organization process related to the dynamics of wave motion. The resulting model, that includes the Harry Dym system, the fractal and fractional operators, has been solved numerically and its stability results have been given. Numerical simulations have proven a dynamic involved in a self-organization process where initial objects are replicated and various fractal patterns are formed. Numerical simulations have also proven that the fractal patterns vary with the fractional order derivative. Hence, this paper improves the preceding works in the domain as it reveals a system capable of artificially structuring the fractal patterns using mathematical concepts.

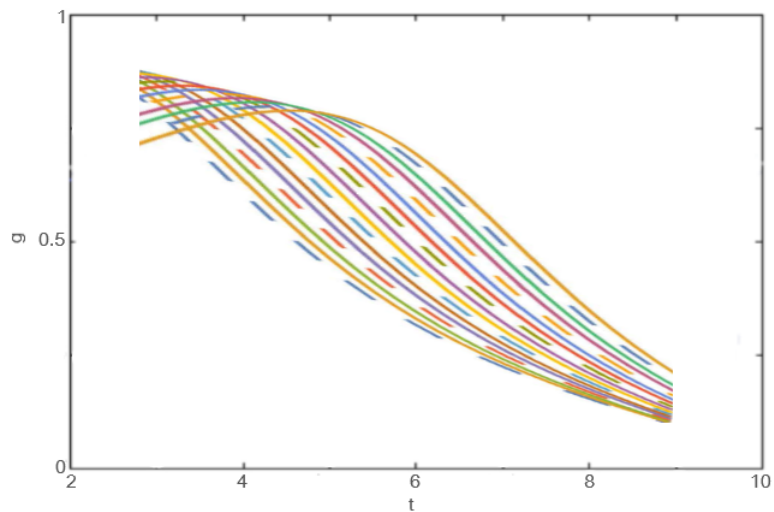


Figure 8: Two-dimensional representation of the solution $g(t, x)$ to model (35)–(36) when $g_0(x) = \frac{6}{10}e^x$ and $\gamma = 1$.

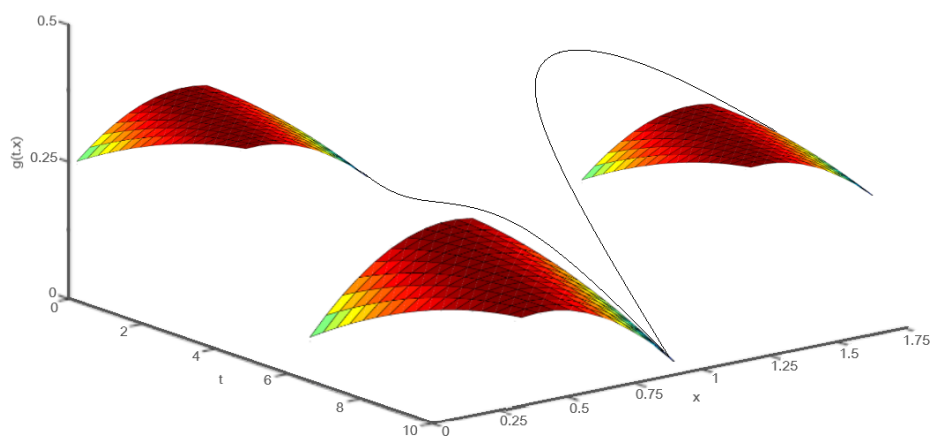


Figure 9: Three-dimensional representation of the solution $g(t, x)$ to model (35)–(36) when $g_0(x) = \frac{6}{10}e^x$ and $\gamma = 0.85$. Here, the dynamic is involved in a self-organization process, which consists of getting a structure in which the initial object is replicated approximately exactly to itself or to a part of itself.

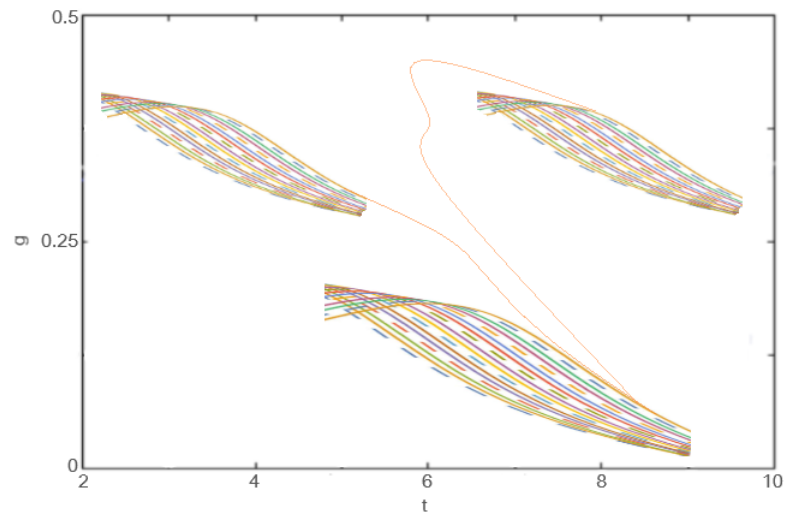


Figure 10: Two-dimensional representation of the solution $g(t, x)$ to model (35)–(36) when $g_0(x) = \frac{6}{10}e^x$ and $\gamma = 0.85$. Here, we can see the projection on the plan (t, g) of the self-organization dynamic.

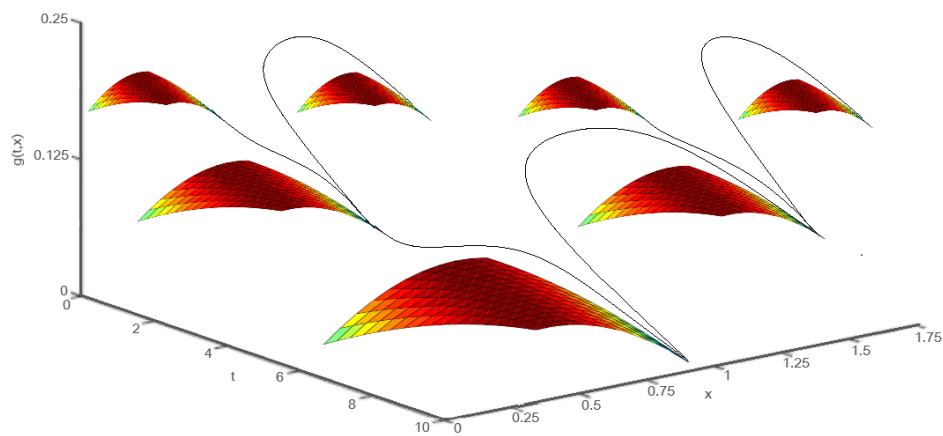


Figure 11: Three-dimensional representation of the solution $g(t, x)$ to model (35)–(36) when $g_0(x) = \frac{6}{10}e^x$ and $\gamma = 0.65$. Here, the self-organization dynamic is maintained and continues further, as it expands and multiplies in a similar way.

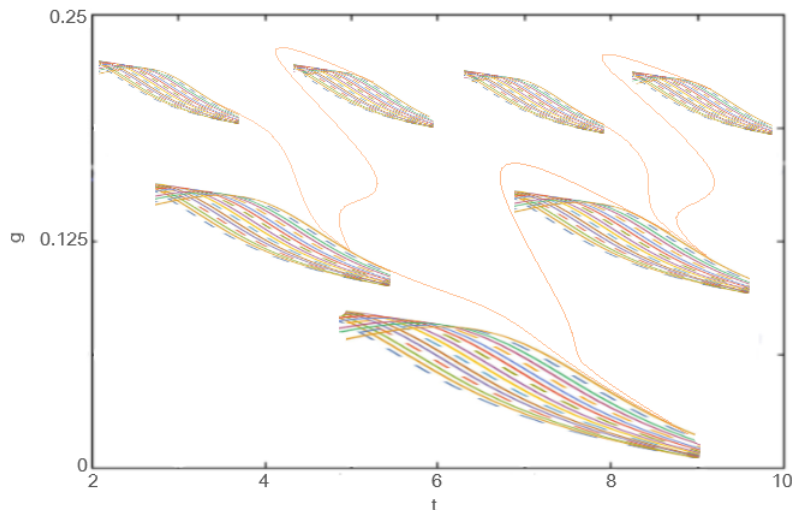


Figure 12: Two-dimensional representation of the solution $g(t, x)$ to model (35)–(36) when $g_0(x) = \frac{6}{10}e^x$ and $\gamma = 0.65$. Here, we can see the projection on the plan (t, g) of the self-organization dynamic that is maintained and continues further, as it expands and multiplies.

References

- [1] E. F. Doungmo Goufo. Application of the Caputo-Fabrizio fractional derivative without singular kernel to Korteweg-de Vries-Burgers equation. *Mathematical Modelling and Analysis* **21** (2) (2016) 188–198.
- [2] C. Rogers. The Harry Dym equation in 2+1 dimensions: A reciprocal link with the Kadomtsev-Petviashvili equation. *Physics Letters A* **120** (1) (1987) 15–18.
- [3] E. Goufo, P. Tchepmo, Z. Ali and A. Kubeka. A comparative analysis of the Harry Dym model with and without singular kernel. *Journal Of Computational Analysis And Applications* **25** (2018) 228–240.
- [4] D. Goufo, E. Franc and S. Kumar. Shallow water wave models with and without singular kernel: existence, uniqueness, and similarities. *Mathematical Problems in Engineering* **2017** (2017) 1–9.
- [5] A. Yokuş and S. Gülbahar. Numerical solutions with linearization techniques of the fractional Harry Dym equation. *Applied Mathematics and Nonlinear Sciences* **4** (1) (2019) 35–42.
- [6] F. Jarad, T. Abdeljawad and Z. Hammouch. On a class of ordinary differential equations in the frame of Atangana-Baleanu fractional derivative. *Chaos, Solitons & Fractals* **117** (2018) 16–20.
- [7] J. Singh, D. Kumar and S. Kumar. An efficient computational method for local fractional transport equation occurring in fractal porous media. *Computational & Applied Mathematics* **39** (3) (2020).
- [8] E. F. Doungmo Goufo. The Proto-Lorenz system in its chaotic fractional and fractal structure. *International Journal of Bifurcation and Chaos* **30** (12) (2020) P. 2050180.
- [9] E. F. Doungmo Goufo. Solvability of chaotic fractional systems with 3D four-scroll attractors. *Chaos, Solitons & Fractals* **104** (2017) 443–451.

- [10] P. Melby, N. Weber and A. Hübler. Dynamics of self-adjusting systems with noise. *Chaos: An Interdisciplinary Journal of Nonlinear Science* **15**(3) (2005) P. 033902.
- [11] S. Hotton and J. Yoshimi. Extending dynamical systems theory to model embodied cognition. *Cognitive Science* **35** (3) (2011) 444–479.
- [12] A. Kumar, S. Kumar and S.-P. Yan. Residual power series method for fractional diffusion equations. *Fundamenta Informaticae* **151** (1-4) (2017) 213–230.
- [13] E. F. Doungmo Goufo. On chaotic models with hidden attractors in fractional calculus above power law. *Chaos, Solitons & Fractals* **127** (2019) 24–30.
- [14] E. F. Doungmo Goufo and J. J. Nieto. Attractors for fractional differential problems of transition to turbulent flows. *Journal of Computational and Applied Mathematics* **339** (2018) 329–342.
- [15] E. F. Doungmo Goufo, S. Kumar and S. Mugisha. Similarities in a fifth-order evolution equation with and with no singular kernel. *Chaos, Solitons & Fractals* **130** (2020) P. 109467.
- [16] E. Babolian and A. Shahsavaran. Numerical solution of nonlinear fredholm integral equations of the second kind using Haar wavelets. *Journal of Computational and Applied Mathematics* **225**(1) (2009) 87–95.
- [17] Ü. Lepik and H. Hein. *Haar Wavelets: With Applications* (Springer Science & Business Media, 2014).
- [18] E. F. Doungmo Goufo. Mathematical analysis of peculiar behavior by chaotic, fractional and strange multiwing attractors. *International Journal of Bifurcation and Chaos* **28** (10) (2018) P. 1850125.
- [19] M. Caputo. Linear models of dissipation whose Q is almost frequency independent–II. *Geophysical Journal International* **13** (5) (1967) 529–539; Reprinted in: *Fract. Calc. Appl. Anal.* **11** (1) (2008) 3–14.
- [20] E. F. Doungmo Goufo. Application of the Caputo-Fabrizio fractional derivative without singular kernel to Korteweg-de Vries-Bergers equation. *Mathematical Modelling and Analysis* **21** (2) (2016) 188–198.
- [21] S. Das. Convergence of Riemann-Liouville and Caputo derivative definitions for practical solution of fractional order differential equation. *International Journal of Applied Mathematics and Statistics* **23** (D11) (2011) 64–74.
- [22] A. A. A. Kilbas, H. M. Srivastava and J. J. Trujillo. *Theory and Applications of Fractional Differential Equations*. Elsevier Science Limited, 2006.
- [23] M. Caputo and M. Fabrizio. A new definition of fractional derivative without singular kernel. *Progr. Fract. Differ. Appl.* **1** (2) (2015) 1–13.
- [24] EF. Doungmo Goufo and Y. Khan. A new auto-replication in systems of attractors with two and three merged basins of attraction via control. *Communications in Nonlinear Science and Numerical Simulation* **96** (2021).
- [25] A. Atangana. Fractal-fractional differentiation and integration: Connecting fractal calculus and fractional calculus to predict complex system. *Chaos, Solitons & Fractals* **102** (2017) 396–406.
- [26] E. F. Doungmo Goufo. Fractal and fractional dynamics for a 3D autonomous and two-wing smooth chaotic system. *Alexandria Engineering Journal* (2020).
- [27] M. Razzaghi and S. Yousefi. The Legendre wavelet operational matrix of integration. *International Journal of Systems Science* **32** (4) (2001) 495–502.
- [28] Y. Chen, X. Ke and Y. Wei. Numerical algorithm to solve system of nonlinear fractional differential equations based on wavelets method and the error analysis. *Applied Mathematics and Computation* **251** (2015) 475–488.